DOI: 10.1002/ejoc.200800667

A Coumarin-Based Chromogenic Sensor for Transition-Metal Ions Showing Ion-Dependent Bathochromic Shift

Weiying Lin,*[a] Lin Yuan,[a] Xiaowei Cao,[a] Wen Tan,[a] and Yanming Feng[a]

Keywords: Sensors / Transition metals / N,O ligands / Charge transfer / Coumarins

Coumarin pyridyl ketone **1** was designed and synthesized as a new chromogenic sensor for transition-metal ions. Remarkably, the chemosensor showed ion discrimination by exhibiting different extents of bathochromic shifts: 118 nm for Cu^{2+}, 80 nm for Ni^{2+}, and 55 nm for Cd^{2+}. This ion-dependent redshift in the visible region allows the selective detection of these three transition-metal ions by the naked eye. Studies of reference compounds and IR and NMR spectroscopy revealed that the pyridyl ketone moiety was the metal-binding site, whereas the carbonyl group on the coumarin moiety did not participate in the metal-binding process.

Introduction

Transition-metal ions play an important role in a wide variety of fields. On the one hand, transition-metal ions such as Cu^{2+} ions are essential in the human body and participate in enzymatic catalysis and gene expression.[1] On the other hand, a high level of transition-metal ions could be toxic to biological systems.[2,3] For instance, high concentrations of Ni^{2+} ions may cause a reduction in plant growth by reducing concentrations of chlorophyll a and b, cytochrome b_6 and b_{559}, and ferrodoxin.[3a,3b] Furthermore, long-term exposure to Cd^{2+} may elicit diseases such as renal dysfunction, reduced lung capacity, and emphysema.[3c,3d] Thus, the detection of transition-metal ions is of significance to the environment, in medicine, and in biology.[4] Considerable efforts have been devoted to the detection of transition-metal ions. Unfortunately, many industrial detection methods rely on time-consuming and sophisticated analytical techniques, such as atomic absorption/emission spectrometry and inductively coupled plasma mass spectroscopy.[5] These are not very suitable for convenient "in-the-field" detection. Therefore, it is very important to develop sensitive, rapid, and simple-to-use methods to sense transition-metal ions. Up to date, many researchers have focused on colorimetric,[6] electrochemical,[7] and fluorescent[8,9] methods in the hope of developing new transition-metal-ion sensors.

Among these methods, colorimetric sensing appeared to be the most attractive for detecting transition-metal ions. As colorimetric sensors normally exhibit color changes upon metal-ion binding, they can be employed for simple naked-eye applications without the use of any expensive equipment. In addition, many paramagnetic transition-metal ions, such as Cu^{2+} and Ni^{2+}, possess intrinsic emission quenching properties, so they often quench organic fluorophore emission.[4,9] Consequently, many fluorogenic sensors only have limited use for transition-metal ions. Thus, colorimetric sensing seems to be more promising in the development of simple-to-use and naked-eye diagnostic tools for transition-metal ions. Although great effort has been made in the field of chromogenic chemosensors, it is still very challenging to design colorimetric chemosensors that show spectroscopic discrimination for transition-metal ions, because the complexes of the receptors to many transition-metal ions usually display very similar absorption profiles.[10]

It is known that by incorporation of an electron-donating group in the 7-position and an electron-withdrawing group in the 3-position the resulting coumarin derivatives have absorption bands well within the visible region as a result of effective intramolecular charge transfer (ICT) induced by the electron push–pull system.[11] Thus, to develop chromogenic sensors that are suitable for naked-eye detection of transition-metal ions, compound **1** (Figure 1), a coumarin derivative with an electron-donating diethylamino group and an electron-withdrawing pyridyl ketone moiety, was designed. A double bond was inserted between the coumarin ring and the pyridyl ketone moiety to afford a highly conjugated compound, so the absorption could further extend into the visible region. We reasoned that the pyridyl ketone could also act as a metal-ion binding site. Thereby, upon binding to a metal ion, the electron-withdrawing capability

[a] State Key Laboratory of Chemo/Biosensing and Chemometrics, College of Chemistry and Chemical Engineering, Hunan University,
Changsha, Hunan 410082, P. R. China
Fax: +86-731-8821464
E-mail: weiyinglin@hnu.cn

Supporting information for this article is available on the WWW under http://www.eurjoc.org or from the author.

of the pyridyl ketone moiety should increase, which leads to stronger ICT. A bathochromic shift in the absorption spectra upon addition of metal ions is thus expected. This redshift behavior should further ensure that the sensor has a chromogenic response in the visible region for naked-eye detection. Additionally, the binding affinity of transition-metal ions usually follows the Irving and Williams order:[10a,12] $Mn^{2+} < Fe^{2+} < Ni^{2+} < Cu^{2+} > Zn^{2+}$. Therefore, the sensor was also envisaged to have some extent of ion selectivity.

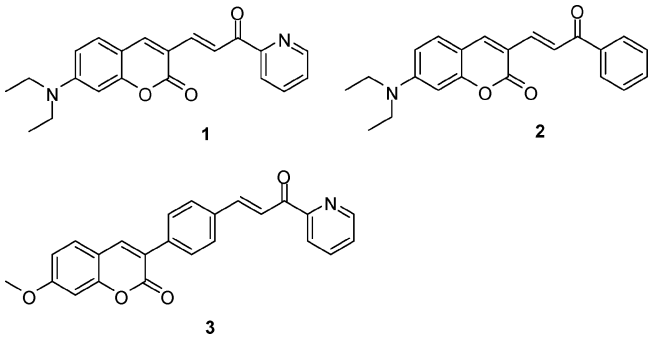

Figure 1. The structures of sensor **1** and reference compounds **2** and **3**.

In this work, coumarin pyridyl ketone **1** was rationally designed and readily synthesized as a new chromogenic sensor for transition-metal ions. Remarkably, the chemosensor showed ion discrimination by exhibiting different extents of bathochromic shifts: 118 nm for Cu^{2+}, 80 nm for Ni^{2+}, and 55 nm for Cd^{2+}. This ion-dependent redshift in the visible region allows the selective detection of these three transition-metal ions by the naked eye. Studies of reference compounds and IR and NMR spectroscopy revealed that the pyridyl ketone moiety was the metal-binding site, whereas the carbonyl group on the coumarin moiety did not participate in the metal-binding process. On the basis of this binding mode, the bathochromic shift in the absorption spectra upon addition of metal ions was rationalized by the ICT. We believe that the rational approach employed herein for the design of the chromogenic sensor showing colorimetric response in the visible region will be readily applicable for the development of other naked-eye chromogenic sensors.

Results and Discussion

Synthesis

Chemosensor **1** was readily obtained in two steps (Scheme 1). The intermediate, 7-diethylaminocoumarin-3-aldehyde (**5**), was prepared on the basis of a known procedure.[13] Reaction of intermediate **5** with 2-acetylpyridine afforded compound **1** in a yield of 30%.[14] The structures of the intermediate and the final product were confirmed by NMR and IR spectroscopy, ESI-MS, and elementary analysis.

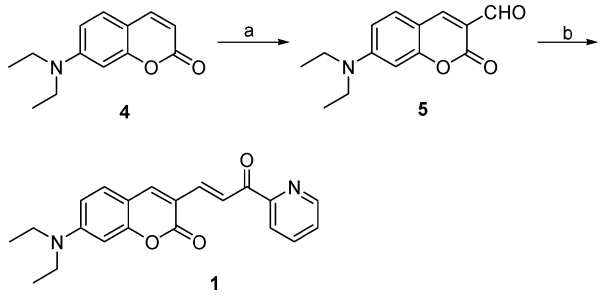

Scheme 1. Synthetic route to compound **1**. Reagents and conditions: (a) $POCl_3$, DMF, 60 °C, 6 h; (b) 2-acetylpyridine, NaOH, ethanol/dimethylbenzene, reflux, 2 h.

Spectral Properties of Sensor 1

As designed, compound **1** displayed an intense absorption band in the visible region peaked at 465 nm, which is redshifted by about 78 nm relative to that of reference compound **4** (Figure 2). This drastic redshift is apparently attributed to ICT. Additionally, compound **1** exhibited a maximum emission around 565 nm. This is 110 nm redshifted relative to that of compound **4**. The redshift in both the absorption and emission indicate that, indeed, 2-acetylpyridine acts as an electron-withdrawing group in the ICT process.

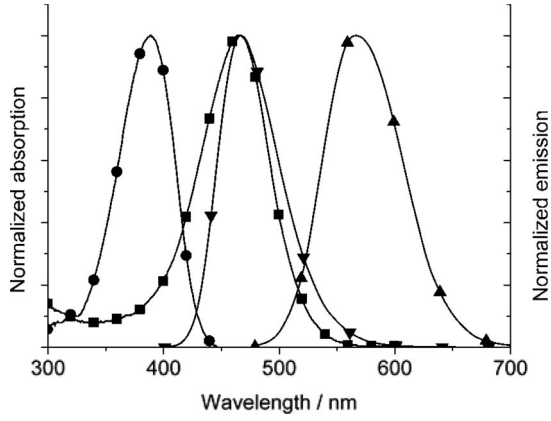

Figure 2. Normalized absorption spectra of **1** (■) and **4** (●) and emission spectra of **1** (▲) and **4** (▼) in CH_3CN/H_2O (95:5).

Sensing Selectivity Studies

Sensor **1** was treated with representative alkali, alkaline earth, and transition-metal ions to evaluate the optical response of the sensor in CH_3CN/H_2O (95:5) or CH_3OH/

H_2O (1:1). As shown in Figure 3a and Table 1, in the presence of 20 equiv. of metal ions such as Ag^+, Fe^{2+}, Na^+, Ca^{2+}, Hg^{2+}, K^+, Mg^{2+}, Mn^{2+}, Na^+, Pb^{2+}, and Zn^{2+}, the absorption spectra of the sensor showed no observable changes. However, a 118 nm redshift in the absorption was observed in the presence of Cu^{2+}. Similarly, Ni^{2+} elicited a redshift in the absorption, but to a different extent, only 80 nm. Satisfactorily, Cd^{2+} in high concentrations (Figure S1) also caused a 55 nm redshift in the absorption spectra. These data suggest that compound **1** could be exploited as a colorimetric sensor for ion discrimination among typical transition-metal ions, such as Cu^{2+}, Ni^{2+}, and Cd^{2+}, which are known to display similar absorption profiles and are thus difficult to differentiate. Indeed, as shown in Figure 4 (for a color version, see Figure S2 in the Supporting Information), the complex of **1** with Cu^{2+}, Ni^{2+}, and Cd^{2+} show the colors of blue, purple, and orange, respectively. Figure S3 displays the absorption ratios (A_{583}/A_{465}) for sensor **1** to different cations. In CH_3OH/H_2O (1:1), the sensor also exhibited a different extent of redshift response to Cu^{2+} and Ni^{2+} (Figure 3b). The fluorescence response of **1** to different metal ions in CH_3CN/H_2O (95:5) is shown in Figure S4. The Cu^{2+} and Ni^{2+} ions quenched the emission but to different extents, whereas most of the other metal ions only slightly influenced the emission.

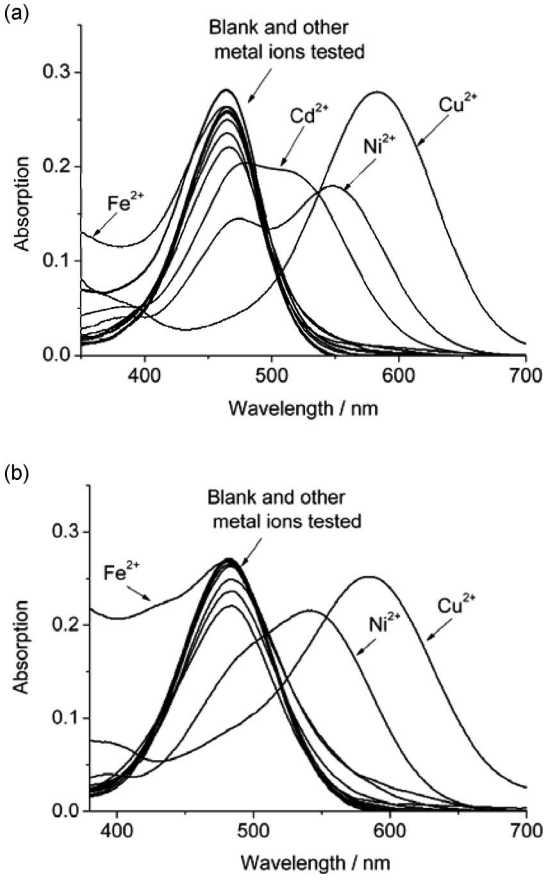

Figure 3. (a) Absorption spectra changes of sensor **1** (10 μM) in CH_3CN/H_2O (95:5) upon addition of 20 equiv. of Ag^+, Ca^{2+}, Fe^{2+}, Cu^{2+}, Hg^{2+}, K^+, Mg^{2+}, Mn^{2+}, Na^+, Ni^{2+}, Pb^{2+}, and Zn^{2+} and 200 equiv. of Cd^{2+}; (b) absorption spectra changes of sensor **1** (10 μM) in CH_3OH/H_2O (1:1) upon addition of various metal ions (100 equiv.) (notably, Fe^{2+} ions have significant absorption in the UV/Vis region and this accounts for the shoulder band appearing from 350 to 480 nm).

Table 1. Absorption spectroscopic data of sensor **1** and its Ni^{2+}, Cu^{2+}, and Cd^{2+} complexes in CH_3CN/H_2O (95:5).

Compound	λ_{max} / nm	ε / $M^{-1}cm^{-1}$[a]	Log K
1	465	26, 300	–
1·Cu	583	28, 000	4.94
1·Ni	545	26, 400	3.84
1·Cd	520	–	2.98

[a] The molar absorptivity of **1**·Cd could not be calculated accurately due to the relatively small binding constant.

Figure 4. Color changes observed on **1** (25 μM) in the presence of metal ions in CH_3CN/H_2O (95:5). From left to right: no ion, Cd^{2+}, Ni^{2+}, Cu^{2+}, Pb^{2+}, Ag^+, Na^+, Mg^{2+}, Hg^{2+}, and Zn^{2+} (20 equiv.). The color version is shown in Figure S2, in the Supporting Information.

Sensing Response of Sensor 1 to Cu^{2+}

The absorption spectra of sensor **1** in the presence of different concentrations of Cu^{2+} ions are displayed in Figure 5. When increasing concentrations of Cu^{2+} ions were introduced in CH_3CN/H_2O (95:5), the absorbance of the peak centered at 465 nm gradually decreased with concomitant appearance of a redshifted peak around 583 nm. Furthermore, two well-defined isosbestic points were observed at 393 and 512 nm, which suggests complex formation. The 118 nm redshift should result in a significant change in the absorption ratios. Indeed, sensor **1** displayed a remarkable enhancement in absorption ratios (A_{583}/A_{565}) from 0.038 to 7.18 upon Cu^{2+} treatment (Figure S3). More importantly, the absorption changes were clearly visible to the naked eye. The yellow color of the sensor solution immediately turned to blue upon addition of Cu^{2+}, which further supported the substantial ratiometric absorption response (Figure 4). In CH_3OH/H_2O (1:1), the sensor also displayed the redshift response to Cu^{2+} (Figure 5b). Figure S5 shows the fluorescent response of the sensor to increasing concentrations of Cu^{2+}. The emission peak of sensor **1** at 565 nm was completely quenched. The quenching constant was calculated to be 9.64×10^4 M^{-1} according to the Stern–Volmer plot (Figure S6a).[15] As expected, the optical changes were reversible, as the addition of ethylenediamine completely reversed the absorption and emission spectra changes (Figure S7). This indicates that compound

1 is a true sensor for Cu^{2+}. Additionally, other competing metal ions including Ni^{2+} show negligible interference in the detection of Cu^{2+} (Table S1).

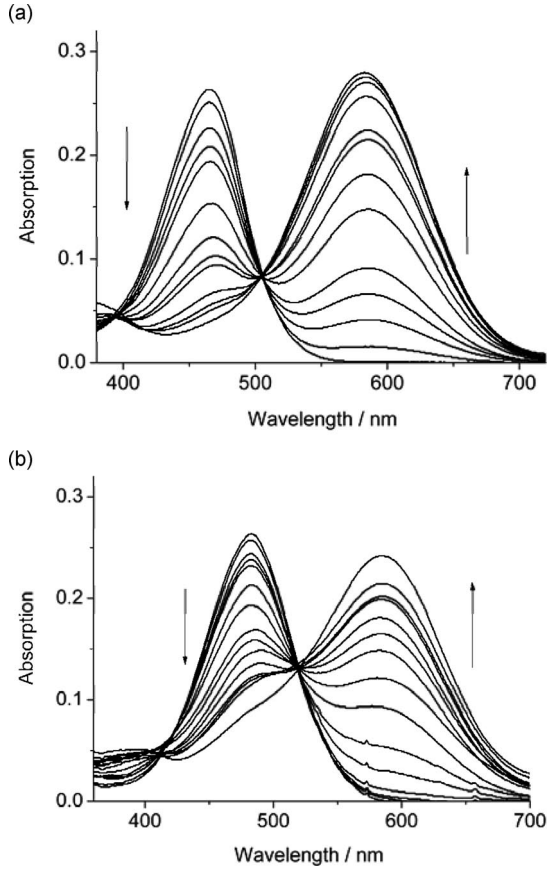

Figure 5. (a) Absorption spectra of sensor **1** (10 μM) in CH_3CN/H_2O (95:5) in the presence of increasing concentration of Cu^{2+} (0–20 equiv.); (b) absorption spectra of sensor **1** (10 μM) in CH_3OH/H_2O (1:1) in the presence of increasing concentration of Cu^{2+}(0–100 equiv.).

Sensing Response of Sensor 1 to Ni^{2+}

In comparison to Cu^{2+}, a similar optical response was observed when the sensor was treated with Ni^{2+} (Figure 6). When increasing concentrations of Ni^{2+} ions were introduced, the absorbance of the peak centered at 465 nm gradually decreased with concomitant appearance of a redshifted peak around 545 nm. In addition, two well-defined isosbestic points were observed at 393 and 492 nm, which indicates formation of a new complex. The large redshift in the absorption spectra suggests that the absorption changes may be observable to the naked eye. Indeed, the yellow color of the sensor solution immediately turned to purple when Ni^{2+} was introduced (Figure 4). In CH_3OH/H_2O (1:1), the sensor also exhibited the redshift response to Ni^{2+} (Figure 6b). Figure S8 displays the fluorescent response of the sensor to increasing concentrations of Ni^{2+}. The sensor emission was significantly quenched by Ni^{2+}, and the quenching constant was determined to be 7.65×10^3 M^{-1} by the Stern–Volmer plot (Figure S6b).[15] Moreover, the addition of ethylenediamine completely reversed the absorption and emission changes (Figure S9), demonstrating the reversible binding nature of the sensor to Ni^{2+}.

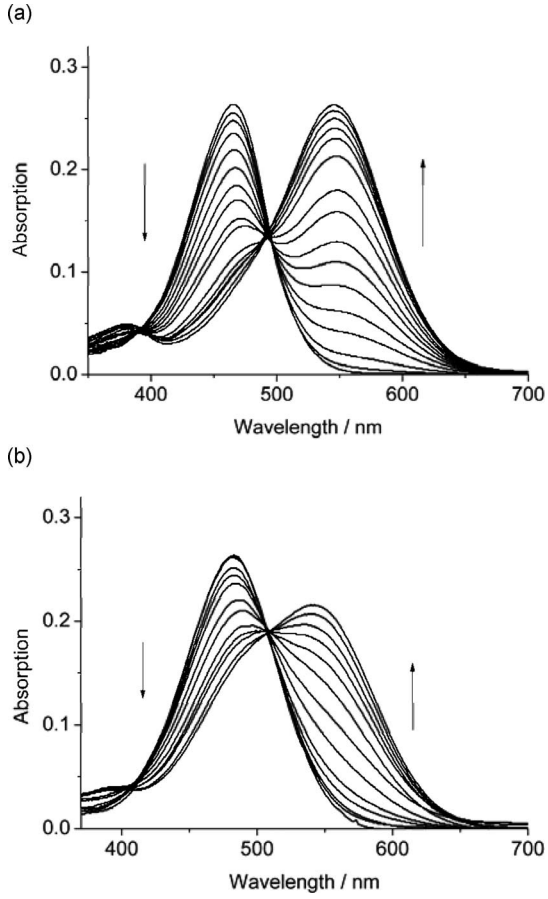

Figure 6. (a) Absorption spectra of sensor **1** (10 μM) in CH_3CN/H_2O (95:5) in the presence of increasing concentration of Ni^{2+} (0–120 equiv.); (b) absorption spectra of sensor **1** (10 μM) in CH_3OH/H_2O (1:1) in the presence of increasing concentration of Ni^{2+} (0–140 equiv.).

Stoichiometry and Binding Constant Studies

To determine the stoichiometry of sensor **1** and metal ions in the complex, the Job's method was employed by keeping the total concentrations of the metal ions and **1** at 50 μM, but varying the molar fraction of the metal ions from 0.1 to 0.9 (Figure S10).[16] Analysis of the Job plot suggests both Cu^{2+} and Ni^{2+} form a 1:1 complex with the sensor. The binding constants ($\log K$) of the sensor with metal ions derived from the Benesi–Hildebrand equation based on a 1:1 binding mode were calculated to be 4.94 for Cu^{2+}, 3.84 for Ni^{2+}, and 2.98 for Cd^{2+} in CH_3CN/H_2O (95:5) (Figure S11).[16b,17] The relative binding affinity of sensor **1** for Cu^{2+}, Ni^{2+}, and Cd^{2+} is in good agreement with the Irving–Williams order.[10a,12]

Binding Mode Studies

Scheme 2 shows the two proposed binding modes of sensor **1** with metal ions. In complex C_1, the metal ion coordi-

nates with the nitrogen atom of the pyridine group and the carbonyl oxygen atom of the pyridyl ketone moiety. By contrast, in complex C_2, the metal ion binds with the nitrogen atom of the pyridine group and the carbonyl oxygen atom of the coumarin moiety.

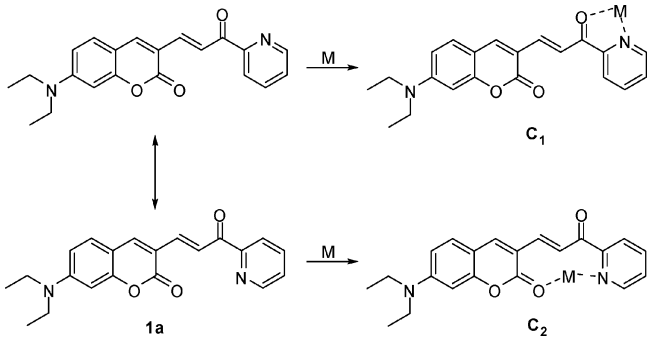

Scheme 2. Possible binding modes of sensor **1** to Cu^{2+}, Ni^{2+}, and Cd^{2+}.

To differentiate these two different binding modes and also examine the role of the nitrogen atom of the pyridine group plays in the binding process, reference compounds **2** and **3** were treated with metal ions. When Ni^{2+} or Cu^{2+} ions were added to compound **2**, which lacks the nitrogen atom

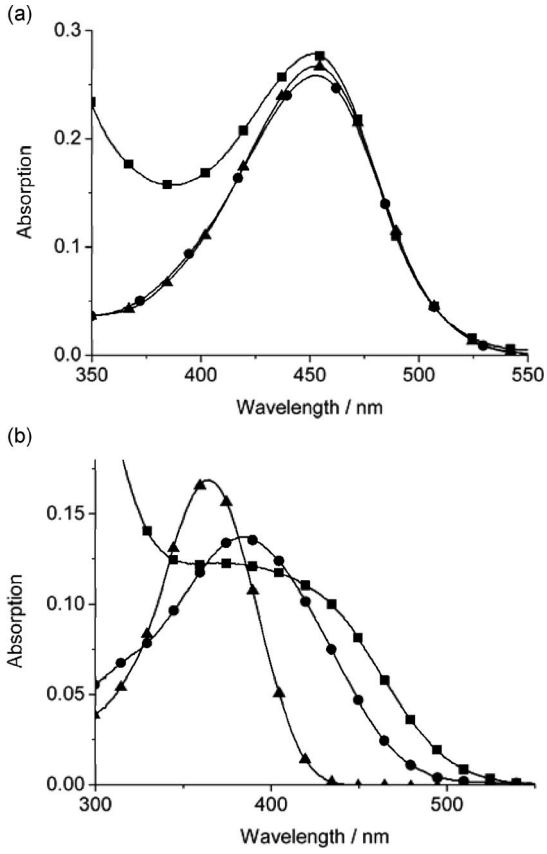

Figure 7. (a) Absorption spectra of reference compound **2** (▲), **2** with Cu^{2+}(■) (20 equiv.), and **2** with Ni^{2+} (●) (50 equiv.) in CH_3CN/H_2O (95:5); (b) absorption spectra of reference compound **3** (▲), **3** with Cu^{2+} (■) (20 equiv.), and **3** with Ni^{2+} (●) (50 equiv.) in CH_3CN/H_2O (95:5).

in comparison to sensor **1**, there were no clear absorption changes observed (notably, 20 equiv. of Cu^{2+} ions have significant absorption in the UV/Vis region and this accounted for the shoulder band appearing from 350 to 400 nm; Figure 7a), implying that the nitrogen atom of the pyridine group of sensor **1** plays a very important role in the interaction with the metal ions. Figure 7b shows the absorption spectra of compound **3** in the absence or presence of metal ions. The absorption spectra of **3** displayed a similar redshift behavior upon addition of the metal ions in comparison to **1**, indicating that **1** and **3** have the same binding mode. As compound **3** has a spacer, a phenyl group, between the pyridyl ketone group and the coumarin moiety, it is unlikely that metal ions will bind with the nitrogen atom of the pyridine group and the carbonyl oxygen atom of the coumarin moiety. Taken together, this evidence suggests that complex C_1 is more probable to be the complex formed between **1** with the metal ion. On the basis of this binding mode, the bathochromic shift in the absorption spectra upon addition of the metal ions can be rationalized by ICT. The coordination of a metal ion to the pyridyl ketone moiety increases its electron-withdrawing character, which leads to a stronger ICT from the electron-donating diethylamino group to the metal-complexed pyridyl ketone moiety. In addition, the different extents of redshift observed in Cu^{2+}, Ni^{2+}, and Cd^{2+} may be explained on the basis that they have different charge densities.[18]

IR and ^{1}H NMR Spectroscopic Studies

To further probe the metal-ion binding site as proposed above, we initially attempted to characterize the structures of metal-ion-bound **1** by crystallographic techniques. Unfortunately, our efforts to obtain the crystal structures were not successful. Accordingly, we decided to employ IR and NMR spectroscopic techniques to further elucidate the coordination mode between **1** and the metal ions. Figure 8 shows the partial IR spectra of sensor **1** before and after the addition of Ni^{2+} and Cu^{2+} ions. The carbonyl group of the lactone on the coumarin moiety and the carbonyl group of the pyridyl ketone moiety show characteristic IR peaks at 1724 and 1655 cm^{-1}, respectively. Upon addition of metal ions, the IR peak corresponding to the carbonyl group of the lactone on the coumarin moiety did not display a marked shift. By contrast, upon the introduction of Ni^{2+} and Cu^{2+} ions, the IR peak corresponding to the carbonyl group of the pyridyl ketone moiety was shifted and merged to the bands centered at 1618 and 1616 cm^{-1} (overlapped with the characteristic IR band of the phenyl group), respectively. These IR data confirmed that the carbonyl group of the pyridyl ketone moiety was involved in the metal coordination, whereas the carbonyl group of the lactone on the coumarin moiety did not participate in the metal-binding process. This is in good agreement with the aforementioned proposed binding mode.

Because Cu^{2+} and Ni^{2+} have paramagnetic character and Cd^{2+} also displayed the bathochromic shift in the absorp-

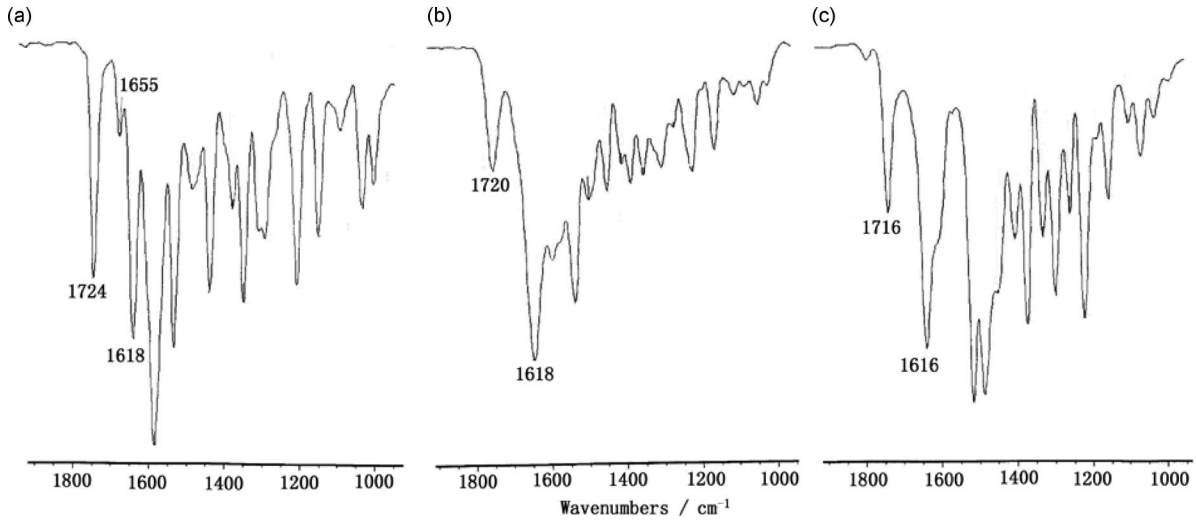

Figure 8. Partial infrared spectra of (a) sensor **1**, (b) **1** with Ni^{2+}, and (c) **1** with Cu^{2+}.

tion spectra upon treatment with the sensor (Figure S1 and Table 1), we used Cd^{2+} as an example to study the binding behavior of the sensor to metal ions by NMR spectroscopy. Changes in the ^1H NMR spectra of sensor **1** before and after the addition of Cd^{2+} are shown in Figure 9. In general, Cd^{2+} induced the well-resolved resonance signals of the sensor molecule to become broad and shifted. For instance, the resonance signal corresponding to the –N=CH proton was shifted downfield from 8.77 to 9.00 ppm upon addition of Cd^{2+}. These changes indicated that indeed the sensor complexed with the metal ions.

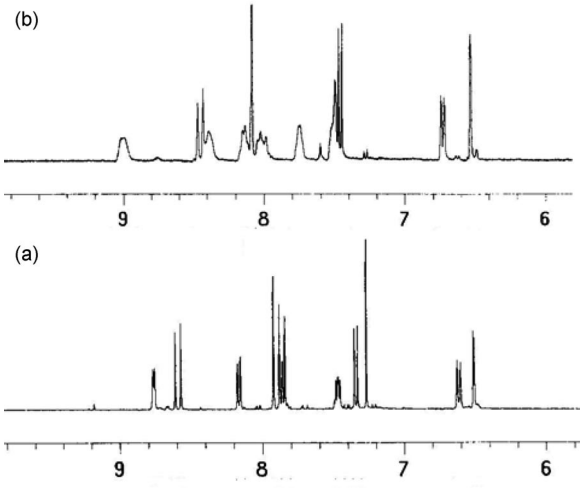

Figure 9. Partial ^1H NMR (400 MHz) spectra of sensor **1** in the absence (a) or presence (b) of Cd^{2+}.

Conclusions

Coumarin **1** was rationally designed and readily synthesized as a new chromogenic sensor for transition-metal ions. Remarkably, the chemosensor showed ion discrimination by exhibiting different extents of bathochromic shifts: 118 nm for Cu^{2+}, 80 nm for Ni^{2+}, and 55 nm for Cd^{2+}. This ion-dependent redshift in the visible region allows the selective detection of these three transition-metal ions by the naked eye. In addition, the relative binding affinity of sensor **1** for Cu^{2+}, Ni^{2+}, and Cd^{2+} is in good agreement with the Irving–Williams order. Furthermore, studies of reference compounds and IR and NMR spectroscopy revealed that the pyridyl ketone moiety was the metal-binding site, whereas the carbonyl group of the lactone on the coumarin moiety did not participate in the metal-ion-binding process. On the basis of this binding mode, the bathochromic shift in the absorption spectra upon addition of metal ions was rationalized by ICT. The coordination of a metal ion to the pyridyl ketone moiety increased its electron-withdrawing character, which led to a stronger ICT from the electron-donating diethylamino group to the metal-complexed pyridyl ketone moiety. We believe that the rational approach employed herein for the design of a chromogenic sensor that shows colorimetric response in the visible region will be applicable for the development of other naked-eye chromogenic sensors.

Experimental Section

General Information and Materials: Unless otherwise stated, all reagents were purchased from commercial suppliers and used without further purification. Solvents used were purified and dried by standard methods prior to use. Twice-distilled water was used throughout all experiments. Melting points were determined with by Beijing taike XT-4 microscopy and are uncorrected. ESI-MS analyses were performed by using a Waters Micromass ZQ-4000 spectrometer. Infrared (IR) absorption spectroscopic analysis was performed with a TENSOR27 spectrometer. Electronic absorption spectra were recorded with a Shimadzu UV-2450 spectrometer. The emission spectra were recorded with a Hitachi F4500 fluorescence spectrophotometer. ^1H spectra were measured with an Inova-400 spectrometer by using TMS as an internal standard. Elementary analysis data were obtained with a Vario El III Elemental Analyzer. TLC analysis was performed on silica gel plates and column chromatography was conducted over silica gel (mesh 200–300), both of which were obtained from Qingdao Ocean Chemicals.

Preparation of Sensor 1: 2-Acetylpyridine (0.12 mL, 1 mmol) and 7-diethylaminocoumarin-3-aldehyde (**5**; 262 mg, 1 mmol) were dissolved in a mixture of ethanol (10 mL) and dimethylbenzene (3 mL) with heating. Then, NaOH (0.03 g) was added, and the solution became red immediately and a precipitate appeared. The reaction solution was heated at reflux for 2 h, and the solvents were then evaporated under reduced pressure. The resulting residue was purified by chromatography on silica (CH_2Cl_2/petroleum ether, 1:1) to give **1** (104.2 mg, 0.301 mmol) in 30.1% yield. M.p. 178–180 °C. IR (KBr): $\tilde{\nu}$ = 3421, 2958, 2925, 2856, 1724, 1655, 1618, 1560, 1512, 1464, 1415 cm^{-1}. ^1H NMR (400 MHz, CD_3OD): δ = 1.24 (t, 6 H), 3.45 (m, 4 H), 6.51 (d, J = 2.4 Hz, 1 H), 6.61 (d, J = 8.4 Hz, 1 H), 7.34 (d, J = 8.8 Hz, 1 H), 7.48 (q, 1 H), 7.85–7.89 (2 H), 7.94 (s, 1 H), 8.17 (d, J = 7.6 Hz, 1 H), 8.60 (d, J = 16 Hz, 1 H), 8.77 (d, J = 4.4 Hz, 1 H) ppm. ESI-MS: m/z = 349.4 $[M + H]^+$. $C_{21}H_{20}N_2O_3$ (348.4): calcd. C 72.40, H 5.79, N 8.04; found C 72.57, H 5.62, N 8.38.

Spectral Measurements: Metal chlorate (Hg^{2+}, Ni^{2+}, Ca^{2+}, Mg^{2+}, Cd^{2+}, Cu^{2+}, Zn^{2+}, Na^+, K^+), nitrate (Ag^+) or sulfate (Fe^{2+}, Mn^{2+}) stock solutions were prepared in twice-distilled water. Sensor **1** was dissolved in CH_3CN or CH_3OH at room temperature to afford the sensor stock solution. Test solutions were prepared by placing 0.5 mL of the sensor stock solution and an appropriate aliquot of each metal stock into a 5 mL volumetric flask, and diluting the solution to 5 mL with CH_3CN/H_2O or CH_3OH/H_2O. The resulting solution was shaken well, and the absorption and emission spectra of the metal complexed were recorded immediately. Unless otherwise noted, for all measurements, the excitation wavelength was at 465 nm, and both the excitation and emission slit widths were 5 nm.

Supporting Information (see footnote on the first page of this article): Detailed experimental procedures and full characterization data for all compounds synthesized, and some spectra of the sensor.

Acknowledgments

Funding was partially provided by the Key Project of Chinese Ministry of Education (No:108167), the Scientific Research Foundation for the Returned Overseas Chinese Scholars, the State Education Ministry (2007-24), and the Hunan University research funds.

[1] For selected examples, see: a) J. J. R. Frausto da Silva, R. J. P. Williams, *The Biological Chemistry of Elements: The Inorganic Chemistry of Life*, Oxford University Press, Oxford, **1993**; b) M. Olivares, M. Gonzalez, *Am. J. Clin. Nutr.* **1998**, *67*, 952S–959S; c) M. C. Linder, M. Hazegh-Azam, *Am. J. Clin. Nutr.* **1996**, *63*, 797S–811S.

[2] For selected examples, see: a) E. Haslam, *Shikimic Acid Metabolism and Metabolites*, John Wiley & Sons, New York, **1993**; b) Z. L. Harris, J. D. Gitlin, *Am. J. Clin. Nutr.* **1996**, *63*, 836S–841S; c) I. H. Scheinberg, I. Sternlieb, *Am. J. Clin. Nutr.* **1996**, *63*, 842S–845S.

[3] For selected examples, see: a) P. M. Kopittke, C. J. Asher, N. W. Menzies, *Plant Soil.* **2007**, *292*, 283–289; b) M. E. Jones, T. C. Hutchinson, *New Phytol.* **1988**, *108*, 451–459; c) B. J. Alloway, E. Steinnes, *Cadmium in Soils and Plant*, Kluwer Academic Publishers, Boston, **1999**; d) G. F. Nordberg, R. F. M. Herber, L. Alessio, *Cadmium in the Human Environment*, Oxford University Press, Oxford, **1992**.

[4] For reviews and books, see: a) J. R. Lakowicz, *Topics in Fluorescence Spectroscopy Vol. 4: Probe Design and Chemical Sensing*, Kluwer Academic Publishers, New York **2002**; b) A. P. de Silva, H. Q. N. Gunaratne, T. Gunnlaugsson, A. J. M. Huxley, C. P. McCoy, J. T. Rademacher, T. E. Rice, *Chem. Rev.* **1997**, *97*, 1515–1566; c) B. Valeur, I. Leray, *Coord. Chem. Rev.* **2000**, *205*, 3–40.

[5] For selected examples, see: a) J. V. Cizdziel, S. Gerstenberger, *Talanta* **2004**, *64*, 918–921; b) S. Diez, J. M. Bayona, *J. Chromatogr., A* **2002**, *963*, 345–351; c) P. Jitaru, F. C. Adams, *J. Chromatogr., A* **2004**, *1055*, 197–207; d) H. Erxleben, J. Ruzicka, *Anal. Chem.* **2005**, *77*, 5124–5128; e) S. Gil, I. Lavilla, C. Bendicho, *Anal. Chem.* **2006**, *78*, 6260–6264; f) C. Fernandez, A. C. L. Conceicao, R. Rial-Otero, C. Vaz, J. L. Capelo, *Anal. Chem.* **2006**, *78*, 2494–2499.

[6] For selected examples, see: a) A. Caballero, R. Martinez, V. Lloveras, I. Ratera, J. Vidal-Gancedo, K. Wurst, A. Tarraga, P. Molina, J. Veciana, *J. Am. Chem. Soc.* **2005**, *127*, 15666–15667; b) I.-T. Ho, G.-H. Lee, W.-S. Chung, *J. Org. Chem.* **2007**, *72*, 2434–2442; c) T. Gunnlaugsson, J. P. Leonard, N. S. Murray, *Org. Lett.* **2004**, *6*, 1557–1560.

[7] For selected examples, see: a) L. P. Singh, J. M. Bhatnagar, *Talanta* **2004**, *64*, 313–319; b) Z. H. Liu, S. Y. Huan, J. H. Jiang, G. L. Shen, R. Q. Yu, *Talanta* **2006**, *68*, 1120–1125.

[8] For selected examples, see: a) G. M. Cockrell, G. Zhang, D. G. VanDerveer, R. P. Thummel, R. D. Hancock, *J. Am. Chem. Soc.* **2008**, *130*, 1420–1430; b) K. Kiyose, H. Kojima, Y. Urano, T. Nagano, *J. Am. Chem. Soc.* **2006**, *128*, 6548–6549; c) R. Métivier, I. Leray, B. Valeur, *Chem. Commun.* **2003**, 996–997.

[9] For selected recent examples, see: a) Y. Q. Weng, F. Yue, Y. R. Zhong, B. H. Ye, *Inorg. Chem.* **2007**, *46*, 7749–7755; b) G. Klein, D. Kaufmann, S. Schurch, J.-L. Reymond, *Chem. Commun.* **2001**, 561–562; c) Y. Zheng, K. M. Gattas-Asfura, V. Konka, R. M. Leblanc, *Chem. Commun.* **2002**, 2350–2351; d) B. C. Roy, B. Chandra, D. Hromas, S. Mallik, *Org. Lett.* **2003**, *5*, 11–14; e) S. Kaur, S. Kumar, *Tetrahedron Lett.* **2004**, *45*, 5081–5085; f) C. B. Murphy, Y. Zhang, T. Troxler, V. Ferry, J. J. Martin, W. E. Jones, *J. Phys. Chem. B* **2004**, *108*, 1537–1543.

[10] For selected examples, see: a) K. Rurack, *Spectrochim. Acta Part A* **2001**, *57*, 2161–2195; b) K. Soroka, R. S. Vithanage, D. A. Phillips, B. Walker, P. K. Dasgupta, *Anal. Chem.* **1987**, *59*, 629–636; c) K. Rurack, R. Radeglia, *Eur. J. Inorg. Chem.* **2000**, 2271–2282.

[11] a) B. Valeur, *Molecular Fluorescence: Principles and Applications*, Wiley-VCH, New York, **2001**, pp. 56–62; b) A. Gocmen, M. Bulut, C. Erk, *Pure Appl. Chem.* **1993**, *65*, 447–450; c) T. Z. Yu, Y. L. Zhao, D. W. Fan, *J. Mol. Struct.* **2006**, *791*, 18–22.

[12] H. Irving, R. J. P. Williams, *Nature* **1948**, *162*, 746–747.

[13] J.-S. Wu, W.-M. Liu, X.-Q. Zhuang, F. Wang, P.-F. Wang, S.-L. Tao, X.-H. Zhang, S.-K. Wu, S.-T. Lee, *Org. Lett.* **2007**, *9*, 33–36.

[14] T. Wang, Y. Zhao, M. Shi, F. Wu, *Dyes Pigm.* **2007**, *75*, 104–110.

[15] a) B. Valeur, *Molecular Fluorescence: Principles and Applications*, Wiley-VCH, New York, **2001**; b) A. Saxena, M. Fujiki, R. Rai, G. Kwak, *Chem. Mater.* **2005**, *17*, 2181–2185; c) A. Saxena, M. Fujiki, R. Rai, S.-Y. Kim, G. Kwak, *Macromol. Rapid Commun.* **2004**, *25*, 1771–1775.

[16] a) W. C. Vosburgh, G. R. Cooper, *J. Am. Chem. Soc.* **1941**, *63*, 437–442; b) W. Lin, L. Yuan, J. Feng, *Eur. J. Org. Chem.* **2008**, 3821–3825.

[17] a) H. A. Benesi, J. H. Hildebrand, *J. Am. Chem. Soc.* **1949**, *71*, 2703–2707; b) T.-L. Kao, C.-C. Wang, Y.-T. Pan, Y.-J. Shiao, J.-Y. Yen, C.-M. Shu, G.-H. Lee, S.-M. Peng, W.-S. Chung, *J. Org. Chem.* **2005**, *70*, 2912–2920; c) I.-T. Ho, G.-H. Lee, W.-S. Chung, *J. Org. Chem.* **2007**, *72*, 2434–2442.

[18] J. Bourson, J. Pouget, B. Valeur, *J. Phys. Chem.* **1993**, *97*, 4552–4557.

Received: July 7, 2008
Published Online: September 3, 2008

